Quadruple-editing of MAPK and PI3K pathways effectively blocks the progression of KRAS-mutated colorectal cancer cells

Zaozao Wang (zaozao83630@bjmu.edu.cn)
Beijing Cancer Hospital

Bin Kang
BGI-Shenzhen: BGI Group

Qianqian Gao
BGI-Shenzhen: BGI Group

Lei Huang
BGI-Shenzhen: BGI Group

Yingcong Fan
Beijing Cancer Hospital

Jianhong Yu
Beijing Cancer Hospital

Jiabo Di
Beijing Cancer Hospital

Beihai Jiang
Beijing Cancer Hospital

Feng Gao
BGI-Shenzhen: BGI Group

Dan Wang
BGI-Shenzhen: BGI Group

Haixi Sun
BGI-Shenzhen: BGI Group

Ying Gu
BGI-Shenzhen: BGI Group

Jian Li
Beijing Cancer Hospital

Xiangqian Su
Beijing Cancer Hospital

Research

Keywords: Quadruple-gene editing, KRAS-mutated colorectal cancer, MAPK pathway, PI3K pathway, ADV-protein complex

Posted Date: February 24th, 2021

DOI: https://doi.org/10.21203/rs.3.rs-230629/v1

Abstract

Background

Mutated KRAS promotes the activation of mitogen-activated protein kinase (MAPK) pathway and the progression of colorectal cancer (CRC) cells. Aberrant activation of phosphatidylinositol 3-kinase (PI3K) pathway strongly attenuates the efficacy of MAPK suppression in KRAS-mutated CRC cells. The development of a novel strategy targeting dual-pathway is therefore highly essential for the therapy of KRAS-mutated CRC cells.

Methods

In this study, a quadruple-depleting system for KRAS, MEK1, PIK3CA, and mammalian target of rapamycin (MTOR) genes based on Clustered Regularly Interspaced Short Palindromic Repeats (CRISPR)/SaCas9 was developed. Serotype 5 of adenovirus (ADV5) was used as packaging virus for systemic delivery of the CRISPR system. To enhance infection efficiency and specificity of ADV5 to CRC cells and reduce its non-specific tissue tropism, two engineered proteins, an adaptor and a protector were synthesized and formed an ADV-protein complex (APC) when delivered the quadruple-editing system intravenously *in vivo*.

Results

The quadruple-editing significantly inhibited MAPK and PI3K pathways in CRC cells with oncogenic mutations of KRAS and PIK3CA or with KRAS mutation and compensated PI3K activation. Compared with MEK and PI3K/MTOR inhibitors, the quadruple-editing induced more significant survival inhibition on primary CRC cells with oncogenic mutations of KRAS and PIK3CA. The adaptor protein which specifically targeting epithelial cell adhesion molecule (EpCAM) could dramatically enhance infection efficiency of ADV5 to CRC cells. and the protector protein could significantly reduce the off-targeting tropisms in a variety of organs. Moreover, the quadruple-editing intravenously delivered by APC significantly blocked dual-pathway and tumor growth, without influencing normal tissues in cell- and patient-derived xenograft models of KRAS-mutated CRC cells.

Conclusions

APC-delivered quadruple-editing of MAPK and PI3K pathways effectively and specifically blocked the progression of KRAS-mutated CRC cells.

Background

Colorectal cancer (CRC) is one of the most commonly diagnosed malignancies, as well as being one of the leading causes of cancer death, accounting for nearly 10% of the total incidence and mortality worldwide [1]. KRAS is the most frequently mutated oncogene in CRC, carrying diverse activating mutations in codon 12/13, including G12D/V/C/S/A/R and G13D/C. The oncogenic mutations of KRAS promote the activation of mitogen-activated protein kinase (MAPK) pathway and cause spontaneous tumor development [2].

Significant efforts have been made to explore KRAS-targeted therapies in the past decades. Although no clinically approved drug has been proposed yet, promising outcomes have been reported in targeting KRAS mutant and other components of MAPK pathway. For instance, AMG 510, a novel KRAS G12C inhibitor, and MEK inhibitors (Pimasertib and AZD6244) exhibited significant anti-tumor activities in early stages of clinical trials [3, 4]. However, the phosphatidylinositol 3-kinase (PI3K)/protein kinase B (AKT)/mammalian target of rapamycin (MTOR) pathway could be stimulated by activating mutations of PIK3CA (E545K and H1047R) [5]. The aberrant activation of PI3K pathway remarkably reduced the therapeutic efficacy of inhibiting MAPK signaling in KRAS-mutated CRC cells [6]. Therefore, dual-inhibition of MAPK and PI3K pathways is required for the complete inhibition of KRAS signaling and tumor progression. However, the overlapping toxicities limit the clinical activities of combined therapy with currently available inhibitors, such as MEK inhibitor (Pimasertib) and PI3K/MTOR inhibitor (Voxtalisib) [7], and MEK inhibitor (AZD6244) and AKT inhibitor (MK2206) [8]. Therefore, development of a novel strategy targeting MAPK and PI3K pathways is highly essential for the treatment of KRAS-mutated CRC cells.

CRISPR (Clustered Regularly Interspaced Short Palindromic Repeats) system has been reported as a potent strategy for efficient gene depletion *in vitro* and *in vivo* based on double-strand break (DSB) repair mechanism at target sites [9]. Moreover, multiplex genome engineering enables simultaneous editing of several sites within the mammalian genome by encoding multiple guide sequences into a single CRISPR array [10, 11]. Recent studies demonstrated that therapeutic strategies based upon multiplex genome editing was powerful to fight against hematopoietic malignancies, which indicated its broad applications in cancer treatment [12, 13]. Compared with the most popular enzyme SpCas9, SaCas9 is remarkably smaller in size and is more appropriate for *in vivo* editing, and has been previously used to rescue vision loss in patients with Leber congenital amaurosis [14, 15]. Furthermore, selective targeting of oncogenic mutations of KRAS, such as G12V/D or G12S by CRISPR/Cas9, has been reported to inhibit the proliferation of tumor cells [16, 17]. However, to date, no study has assessed the effects of multiple targeting of KRAS and downstream signaling pathways.

One bottleneck undermining the application of genome-editing techniques to treat cancer is the lack of an *in vivo* efficient and safe delivery method. The human adenovirus serotype 5 (ADV5) is widely used in gene therapy of cancer due to its high infection efficiency and high expression levels of therapeutic genes [18]. However, the current method of ADV5 administration is only local injection because of the non-specific tissue tropism and toxicity, especially in liver, under a systemic delivery. A previous research demonstrated that engineered proteins might be promising to overcome this challenge. For instance, an

adaptor protein, consisting of a single-chain variable fragment (scFv) antibody against human epidermal growth factor receptor 2 (HER2), has shown to retarget ADV5 to the HER2-positive breast cancer cells and enhance the targeting specificity [19]. Besides, a scFv antibody against the hexon protein on ADV5 surface could attenuate its interaction with coagulation factor X (FX), and reduce its off-targeting tissue tropism as well [20].

In the present study, we constructed a CRISPR/SaCas9 system, simultaneously depleting four components of MAPK and PI3K pathways, such as KRAS, MEK1, PIK3CA, and MTOR. In addition, we developed two engineered proteins, an adaptor and a protector, to facilitate the intravenous delivery of CRISPR system in ADV5 vector to the CRC cells over-expressing epithelial cell adhesion molecule (EpCAM). The quadruple-depletion of MAPK and PI3K pathways effectively inhibited the progression of KRAS-mutated CRC cells *in vivo*, and might be a novel therapeutic strategy for CRC.

Methods

CRC tumor samples

In the current study, seven tumor tissues collected from patients with CRC who underwent radical surgery at Peking University Cancer Hospital & Institute (Beijing, China) were used to isolate primary tumor cells and establish PDX models. This study was approved by the Ethics Committee of Peking University Cancer Hospital & Institute (Approval No. 2015KT71), and all participants signed the written informed consent forms prior to commencing the study.

Vector construction

The lentiviral vector of gene depletion, Lenti-CMV::SaCas9-2A-GFP;U6::BsaI-sgRNA, was constructed by the Gateway recombination reaction between the donor vector containing synthetic SaCas9-2A-GFP and sgRNA expressing elements flanked by attL sequences and the destination vector containing attR sequences, pLEX_305 (#41390; Addgene, Watertown, MA, USA). The most efficient sgRNA was chosen from Benchling tool (https://benchling.com), and inserted into the BsaI sites after annealing. The sequences of sgRNAs and matched PAMs were summarized in Additional File 1: Table S1. The scrambled gRNA non-existed in human and mouse genome was cloned into non-target control vector (NT) (5’ GGCACTACCAGAGCTACTCA 3’). The multiplexed vectors were constructed through Golden Gate ligation of corresponding sgRNA cassettes. The plasmids expressing adaptor and protector proteins were respectively constructed by cloning the synthesized coding sequences of adaptor (the ectodomain of CXADR, a phage T4 fibritin polypeptide and a humanized anti-EpCAM/MUC1 scFv), and protector (a humanized anti-hexon scFv and a phage T4 fibritin polypeptide) into pENTER plasmids using restriction sites of Asis□and Xho□. The cloning primers were presented in Additional File 1: Table S2. The adenoviral vector of gene depletion was constructed by the Gateway recombination reaction between the donor vector containing synthetic SaCas9-2A-GFP and sgRNA expressing elements flanked by attL sequences and the destination vector pAdeno-MCMV containing attR sequences. The diagrams of lentiviral and adenoviral vectors were shown in Additional File 2: Figure S1A-1B.

Sanger sequencing and WES

The mutation status of KRAS and PIK3CA in 293T and primary tumor cells was detected by Sanger sequencing. The PCR primers of Sanger sequencing were listed in Additional File 1: Table S2. The on-target and off-target mutations in tumor cells and tissues induced by quadruple-depletion were analyzed by WES. The genomic DNA was fragmented using a Covarias sonication system to mean size of 500-bp. Libraries were constructed after fragmentation, ligated with Ad153 2B Adapters, and then, captured with human whole exome V4 Kit. All the constructed libraries were sequenced on BGI-Seq500 platform using two 100-bp paired-end reads. Somatic SNVs and INDELs were identified by Bamcount tool.

T7E1 assay

The DNA fragment containing breakpoint was PCR amplified, and digested by T7 endonuclease I (NEB) after annealing. The editing efficiencies of sgRNAs were determined by quantifying gel bands via ImageJ software (National Institutes of Health, Bethesda, MD, USA).The PCR primers for T7E1 assay were also listed in Additional File 1: Table S2.

Packaging lentivirus and adenovirus

The lentiviral vector and lentiviral packaging plasmids VSVG and psPAX2 (#8454 and #12260, Addgene) were co-transfected into HEK293T cells through calcium phosphate precipitation. The lentivirus was pelleted by centrifugation at 25000 rpm for 2 h at 4 ℃, and was resuspended using Roswell Park Memorial Institute (RPMI)-1640 medium and stored at -80 ℃. The serotype 5 of adenovirus was packaged and supplied by Obio Technology Co., Ltd. (Shanghai, China). The virus was grown in HEK293T cells, and purified by a two-step CsCl-ethidium bromide gradient ultracentrifugation. The virus titration was determined through IHC of Capsid protein in HEK293T cells.

Establishment of CDX and PDX mouse models of CRC

Here, 5×10^6 cells (HCT116 and SW620) were subcutaneously injected into nude mice to establish the CDX model. Then, the frozen specimens of passage 5 PDX tumor of CRC-PDX01 were thawed and subcutaneously injected into non-obese diabetic severe combined immunodeficient (NOD-SCID) mice to establish the PDX models of passage 6. Once the tumor volume reached 50 – 100 mm^3 as measured with calipers, mice were used for genome editing experiments. All the experiments were approved by the Animal Ethics Committee of Peking University Cancer Hospital & Institute, and performed in full compliance with the Experimental Animal Management Ordinance produced by the Peking University Cancer Hospital & Institute.

Tissue digestion and cell isolation

The primary CRC and PDX tumor tissues were cut into small pieces and digested by incubation for 40 min at 37 ℃ in Dulbecco's modified Eagle's medium (DMEM), containing collagenase type II (50 μg/ml; Sigma-Aldrich, St. Louis, MO, USA), DNase I (20 U/ml; Roche, Basel, Switzerland), and Penicillin–

Streptomycin (1:500; Beijing Solarbio Science & Technology Co., Ltd., Beijing, China). After dissociation, the cell suspensions were filtered through a 70-μm cell strainer (BD Biosciences, Franklin Lakes, NJ, USA) and erythrocytes were removed using 2 ml Red Blood Cell Lysis Buffer (TBD Sciences Inc., Waltham, MA, USA). The isolated tumor cells were stored in liquid nitrogen for the testing of cell viability.

Cell viability, proliferation, and Transwell assays

Fifty thousand primary tumor cells were infected with lentivirus for gene depletion, and the cell viability was assessed by using CellTiter-Glo® 2.0 kit (Promega, Madison, WI, USA) after 48 h according to the manufacturer's instructions. MEK inhibitor (AZD6244) and PI3K/MTOR inhibitor (BEZ235) were purchased from Selleck Chemicals LLC (Houston, TX, USA). The IC50 of AZD6244 or BEZ235 in CRC cells was calculated using GraphPad software. The cell proliferation was assessed using a commercial Cell Counting Kit-8 CCK-8 (Dojindo Molecular Technologies, Inc., Rockville, MD, USA) according to the manufacturer's instructions. Cell migration assay was performed using a Boyden chamber that contained a polycarbonate filter with an 8-μm pore size (Costar Inc., New York, NY, USA). Serum-free DMEM was added to the upper chamber, while complete medium containing 10% fetal bovine serum (FBS) was added to the lower chamber. After transfection, 2×10^5 HCT116 and SW620 cells were separately seeded into the upper chamber and incubated for 48 h. The migrated cells were stained with crystal violet, and five random fields were captured by a microscope. Cell invasion was similarly detected except that the upper chamber was pre-coated with Matrigel (5 mg/ml; BD Biosciences, Franklin Lakes, NJ, USA). All experiments were performed in triplicate.

Western blotting analysis

CRC cells were harvested 48 h after transfection of CRISPR vectors or MEK as well as PI3K/MTOR inhibitor treatments. Proteins were extracted from cells or tumor tissues using RIPA lysis buffer containing complete protease inhibitor cocktail (Roche, Basel, Switzerland). The extracts were separated by sodium dodecyl sulfate-polyacrylamide gel electrophoresis (SDS-PAGE) and transferred onto polyvinylidene fluoride (PVDF) membranes. Membranes were blocked with 5% non-fat milk or 5% bovine serum albumin (BSA), followed by incubation with primary antibodies against the following antigens: KRAS (#12063-1; Proteintech, Rosemont, IL, USA), PIK3CA (#4249; Cell Signaling Technology, Danvers, MA, USA), AKT (#2920; Cell Signaling Technology), phospho-AKT (Ser473; #4060; Cell Signaling Technology), MTOR (#2983; Cell Signaling Technology), S6K (#9202; Cell Signaling Technology), phospho-S6K (T389; #9205; Cell Signaling Technology), MEK (#9126; Cell Signaling Technology), ERK (#4695; Cell Signaling Technology), phospho-ERK (Thr202/Tyr204; #4370; Cell Signaling Technology), and b-Actin (#66009-1; Proteintech). After overnight incubation with primary antibodies at 4 ℃, PVDF membranes were washed three times with TBST, incubated with horseradish peroxidase (HRP)-conjugated goat anti-mouse IgG or goat anti-rabbit IgG secondary antibodies for 1 h at room temperature, and then washed with TBST three times. The immunoreactive bands on the membranes were visualized using an enhanced chemiluminescence detection kit (Millipore, Burlington, MA, USA). The ImageJ

software was used for image processing of band intensity, and relative protein expression levels were normalized to β-actin.

IHC

Formalin-fixed paraffin-embedded CDX and PDX tumor tissues were cut into 4-μm sections. After deparaffinization and rehydration, slices were placed in a citrate buffer solution (pH=6.0) for antigen retrieval, and underwent inhibition and blockage of endogenous peroxidase activity. Sections were incubated with primary antibodies overnight at 4 ℃, followed by processing with a polymer horseradish peroxidase detection system (PV-9000, Zhongshan Goldenbridge Biotechnology). The primary antibodies of KRAS, MEK1, PIK3CA and MTOR were the same as Western blotting, and the primary antibody for Ki67 was purchased from Abcam (#ab16667). The expression levels were evaluated by H-score method. Scoring was independently reviewed by two experienced pathologists.

Hematoxylin and eosin (H&E) staining

Formalin-fixed paraffin-embedded CDX and PDX tumor tissues of vital organs, including liver, lung, kidney, and colon were cut into 4-μm sections. Slices were further processed and stained with H&E. Histopathology was reviewed by an experienced pathologist.

RT-qPCR

Total RNA was extracted using TRIzol reagent (Invitrogen, Carlsbad, CA, USA), and transcribed with TransScript First-Strand cDNA Synthesis SuperMix (#AE301-02; Transgene Biotech Co., Ltd., Beijing, China). Subsequently, RT-qPCR was performed with GoTaq qPCR Master Mix (#A6001; Promega). The relative expression levels of genes were normalized to β-actin. The qPCR primers used to detect mRNA levels of EpCAM, MUC1, and SaCas9 were listed in Additional File 1: Table S2.

Protein expression and purification

The adaptor proteins EpCAM and MUC1, the truncated adaptor protein losing scFv fragment, and the protector protein with His tags were respectively expressed in HEK293T cells. The proteins were extracted using RIPA buffer, purified with Ni-NTA beads (Byeotime), and rinsed with phosphate-buffered saline (PBS) and Amicon Centrifugal Filters (10kDa NMWL, Millipore).

FACS analysis

In order to detect GFP expression, cells harvested were resuspended in 0.22 μm-filtered Dulbecco's phosphate-buffered saline (DPBS), and triplicate measurements from independent samples were analyzed with the CytExpert 2.3 software (Beckman Coulter, Brea, CA, USA).

In vivo genome editing

The adenovirus was pre-incubated with the adaptor and protector proteins (1.0×10^{-7} pmol) at room temperature for 2 h, and injected into the tail veins of CDX and PDX mouse models for two rounds with a 12-day interval. The number of viral particles was 7.0×10^{9}. The tumor size and weight were measured every 3 days.

Statistical analysis

Statistical analysis was carried out respectively by two-tailed Student's t-test and two-way analysis of variance (ANOVA) using SPSS 20.0 (IBM, Armonk, NY, USA) and GraphPad Prism 5.0 (GraphPad Software Inc., San Diego, CA, USA) software. The Kolmogorov-Smirnov test was employed to indicate whether samples were normally distributed. The statistical significance was presented as * $0.01 \leq P < 0.05$, ** $0.001 \leq P < 0.01$, *** $P < 0.001$.

Results

Single and multiple-editing vectors were constructed to target MAPK and PI3K pathways

In order to obtain an effective dual-inhibition of MAPK and PI3K pathways, four important components of MAPK and PI3K pathways (KRAS, MEK1, PIK3CA, and MTOR) were selected for depletion (Figure 1A). The most efficient single guide RNAs (sgRNAs) of CRISPR/SaCas9 system for these four genes were selected by using Benchling tool (https://benchling.com). Moreover, the vectors required for single and multiple depletions were respectively constructed through Golden Gate ligation of corresponding sgRNA cassettes. In addition to single-editing vectors, the multiple-editing vectors included double-depletion of KRAS and MEK1 (KM-KO), and PIK3CA and MTOR (PM-KO), as well as quadruple-depletion of the four genes (KMPM-KO) were constructed (Figure 1B). According to the results of T7E1 assay of HEK293T cells, the vectors of selected single gRNAs (labeled as #1 in Figure 1C-1F) could edit the corresponding gene sites more efficiently compared with those carrying non-overlapping gRNAs targeting the same genes (labeled as #2 in Additional File 3: Figure S2). Moreover, all the vectors with double and quadruple gRNAs could efficiently edit the corresponding targets, with efficiencies ranging from 44.7% to 56.6% (Figure 1G-1I). The expression levels of four gRNAs and the corresponding mutation statuses of KRAS, MEK1, PIK3CA, and MTOR were respectively confirmed by quantitative reverse transcription-polymerase chain reaction (RT-qPCR) and Sanger sequencing in HEK293T cells with quadruple-depletion (KMPM-KO). The abundances of the four gRNAs were almost comparable at the mRNA level, and those could efficiently induce on-target mutations of the corresponding genes (Additional File 4: Figure S3 and Figure 1J). Therefore, the single- and multiple-editing vectors targeting MAPK and PI3K pathways were successfully constructed, and they could be used to investigate the editing effects of dual-pathway on CRC cells.

Quadruple-editing of KRAS, MEK1, PIK3CA, and MTOR efficiently inhibited MAPK and PI3K pathways in CRC cells with oncogenic mutations of KRAS and PIK3CA

About 50% of CRC cells with oncogenic mutation of KRAS simultaneously carried the activating-mutation of PIK3CA [21]. The oncogenic mutations of KRAS (G12D/V/C/S/A/R, G13D/C) and PIK3CA (E545K and

H1047R) could induce the aberrant activation of MAPK and PI3K pathways and progression of CRC cells [2]. Thus, we first detected the effects of single- and multiple-editing of KRAS, MEK1, PIK3CA, and MTOR on HCT116 cells with oncogenic mutations of KRAS (G13D) and PIK3CA (H1047R), comparing with the effects of inhibitors of MAPK and PI3K pathways. The half maximal inhibitory concentration (IC50) values of MEK inhibitor (AZD6244) and PI3K/MTOR inhibitor (BEZ235) in HCT116 cells were respectively 1.0 mM and 2.0 mM (Figure 2A-2B). According to the results of Western blotting on HCT116 cells with single- and multiple-editing, the protein levels of the four target genes were significantly down-regulated by the corresponding editing vectors (Figure 2C-2E). Single- and double-depletion of KRAS and MEK1 (KRAS-KO, MEK1-KO, and KM-KO), and the treatment of AZD6244 down-regulated the phosphorylation level of extracellular signal-regulated kinase (ERK), a downstream component of MAPK pathway, while did not affect the phosphorylation level of AKT, an important component of PI3K pathway. The down-regulation of p-ERK by KM-KO was accompanied with effects similar to those of AZD6244 treatment, and was more significantly noticeable than the effects of KRAS-KO and MEK1-KO (Figure 2C). In contrast, single- and double-depletion of PIK3CA and MTOR (PIK3CA-KO, MTOR-KO, and PM-KO), and the treatment of BEZ235 down-regulated the phosphorylation levels of AKT and S6K, two important components of PI3K pathway, whereas did not influence the phosphorylation level of ERK. The down-regulation of p-AKT and p-S6K by PM-KO showed effects similar to those of BEZ235 treatment, and were more markedly noticeable than the effects of PIK3CA-KO and MTOR-KO (Figure 2D). Furthermore, quadruple-depletion of the four target genes (KMPM-KO) significantly down-regulated the phosphorylation levels of ERK, AKT, and S6K, which were similar to the effects of combining treatment of AZD6244 and BEZ235 (Figure 2E). These results revealed that inhibitory effect of gene editing on the corresponding signaling pathway was specific. The inhibitory effects of double-editing were more noticeable than those of single-editing when a pathway was targeted. Quadruple-editing of KRAS, MEK1, PIK3CA, and MTOR could efficiently and specifically inactivate both MAPK and PI3K pathways. Correspondingly, KMPM-KO also significantly inhibited the proliferation, migration, and invasion of HCT116 cells, with a greater inhibitory effect than single- and double-depletion (Figure 2F-2G). Therefore, quadruple-editing of MAPK and PI3K pathways effectively inhibited the malignant phenotypes of CRC cells with oncogenic mutations of KRAS and PIK3CA.

Quadruple-editing of KRAS, MEK1, PIK3CA, and MTOR effectively blocked the compensated PI3K activation in KRAS-mutated CRC cells with MAPK suppression

A previous research showed that RTK-dependent activation of PI3K pathway was a resistant mechanism against the suppression of MAPK pathway in CRC cells with KRAS mutation and wild-type PIK3CA (Figure 1A) [5]. In order to indicate whether the gene editing of MAPK pathway can induce compensated PI3K activation, we first determined the IC50 value of AZD6244 in SW620 cells with KRAS G12V mutation and wild-type PIK3CA. The IC50 value of AZD6244 in SW620 cells was 1.0 mM (Figure 3A). Then, the activation status of MAPK and PI3K pathways in SW620 cells with AZD6244 treatment and single- and double-depletion of MAPK pathway (KRAS-KO, MEK1-KO, and KM-KO) was detected by Western blotting. As shown in Figure 3B and 3C, similar to AZD6244 treatment, the single- and double-depletion significantly reduced the phosphorylation level of ERK and enhanced the phosphorylation level of AKT.

The up-regulation of p-AKT by KM-KO was more noticeable than that by KRAS-KO and MEK1-KO (Figure 3C). The above-mentioned findings suggested that the gene editing of MAPK pathway also induced compensated PI3K activation in KRAS-mutated CRC cells. In contrast, single- and double-depletion of PIK3CA and MTOR (PIK3CA-KO, MTOR-KO, and PM-KO) remarkably down-regulated the expression levels of p-AKT and p-S6K, while did not affect the expression level of p-ERK. The down-regulated expression levels of p-AKT and p-S6K by PM-KO were more notable than those by PIK3CA-KO and MTOR-KO (Figure 3D). Furthermore, quadruple-depletion of the four target genes (KMPM-KO) significantly down-regulated the expression levels of p-ERK, p-AKT and p-S6K (Figure 3E). Thus, quadruple-editing of KRAS, MEK1, PIK3CA, and MTOR could efficiently block the compensated activation of PI3K pathway under MAPK suppression. Correspondingly, KMPM-KO also markedly inhibited the proliferation, migration, and invasion of SW620 cells, with a greater inhibitory effect than single- and double-depletion of either MAPK or PI3K pathway (Figure 3F-3G). Therefore, compared with only suppressing MAPK pathway, quadruple-editing of MAPK and PI3K pathways could enhance the anti-tumor effects on KRAS-mutated CRC cells through inhibiting the compensated PI3K activation.

In summary, the tumor-suppressive effects of quadruple-editing of KRAS, MEK1, PIK3CA, and MTOR were superior to those of single- and double-editing of MAPK or PI3K pathway in CRC cells with oncogenic mutations of KRAS and PIK3CA or with KRAS mutation and compensated PI3K activation.

Quadruple-editing inhibited the survival of primary CRC cells with diverse mutations of KRAS and PIK3CA

To further confirm the anti-tumor effects of quadruple-editing on CRC cells, the cells of primary tumors and patient-derived xenografts (PDXs) were isolated. Their mutation statuses at hot spots of KRAS and PIK3CA genes, including exon-2 of KRAS, as well as exon-10 and exon-21 of PIK3CA, were detected by Sanger sequencing. Four primary tumor cells and three PDX tumor cells with different types of KRAS mutations or oncogenic mutations of KRAS/PIK3CA were studied. The pathological and mutation data of the seven CRC cases were summarized in Additional File 1: Table S3. These tumor cells were respectively infected with the lentivirus of quadruple-editing, MEK inhibitor (AZD6244), and PI3K/MTOR inhibitor (BEZ235). The inhibition rates of cell survival under various treatments compared with non-treated controls were presented in Figure 4A-4C and 4E-4H. In all the seven cases, quadruple-editing led to a more remarkable inhibition of cell survival than a single-treatment with AZD6244 or BEZ235, and showed similar or more significant inhibitory effects to those of combined therapies. Furthermore, Western blotting results indicated that quadruple-editing of KRAS, MEK1, PIK3CA, and MTOR could efficiently inactivate MAPK and PI3K pathways in primary CRC cells carrying KRAS/PIK3CA double mutations (CRC-P01) or KRAS single mutation (CRC-PDX01). The inhibitory effects of quadruple-editing were more noticeable than those of single-treatment with AZD6244 and BEZ235, and were similar or a little superior to those of combined therapies (Figure 4D and 4I). The above-mentioned results suggested that quadruple-editing had prevalent anti-tumor effects on KRAS-mutated CRC cells.

The complex combining ADV5 and engineered proteins intravenously delivered CRISPR system to CRC with high efficiency and specificity

The ADV5 is extensively utilized in gene therapy of cancer. However, the current administration of ADV5 is only local injection because of its off-target tissue tropism under a systemic delivery. Thus, two proteins, an adaptor and a protector, were engineered to make ADV5 as a proper vector for the intravenous delivery of CRISPR system to CRC. ADV5 infected host cells through a high-affinity interaction between the knob domain of the viral fiber proteins and coxsackievirus and adenovirus receptor (CXADR) displayed on the target cell surface [22]. Therefore, the adaptor protein was composed of the ectodomain of ADV receptor CXADR of cells (ECXADR), and a humanized single-chain variable fragment (scFv) recognizing a certain surface marker on CRC cells, which could be linked by a phage T4 fibritin polypeptide. Adaptor protein could interact with the knob protein of ADV5 fiber through ECXADR domain, and retarget ADV5 to CRC cells through scFv (Figure 5A) [19]. In addition, a scFv antibody against the hexon protein on ADV5 surface was fused to a phage T4 fibritin polypeptide to form a protector protein, which could cover ADV5 to reduce the tissue off-targeting (Figure 5A) [20]. The fibritin induced the trimerization of adaptor and protector proteins, and up-regulated their affinities with ADV5 (Figure 5A) [19, 20].

EpCAM is a transmembrane glycoprotein mediating Ca^{2+}-independent homotypic cell–cell adhesion in epithelia. It has an extremely high rate of over-expression (≥80%) in CRC cells [23, 24]. The results of RT-qPCR showed that compared with 293T cells, EpCAM was over-expressed in 4 human CRC cell lines, including HCT116, LOVO, SW480, and SW620, and in seven types of CRC cells isolated from primary and PDX tumors (Figure 5B-5C). In contrast, Mucin 1, cell surface associated (MUC1), showed lower expression levels in CRC cell lines and primary tumor cells compared with EpCAM (Figure 5B-5C). Therefore, an adaptor protein targeting EpCAM was constructed to enhance the infection efficiency of ADV5 to CRC cells, and a MUC1 adaptor was also developed as a control to confirm the function of the adaptor protein.

In order to validate the function of adaptor protein *in vitro*, the green fluorescent protein (GFP)-expressing ADV5 was pre-incubated with various amounts of EpCAM adaptor protein, or a truncated adaptor protein losing an anti-EpCAM scFv fragment and remaining only ECXADR domain as well as fibritin, and then, infected SW620 cells. The fluorescence-activated cell sorting (FACS) analysis revealed that EpCAM adaptor protein gradually up-regulated the infection efficiency of ADV5 in SW620 cells when increasing amount of protein was pre-incubated with ADV5. However, the truncated adaptor protein gradually down-regulated the infection efficiency of ADV5 in SW620 cells when the amount of protein increased (Additional File 5: Figure S4). The results indicated that EpCAM adaptor protein blocked the interaction between ADV5 and its receptor CXADR through ECXADR domain, and retargeted the virus to EpCAM protein on CRC cells by anti-EpCAM scFv. Afterwards, the GFP-expressing ADV5 was respectively pre-incubated with various amounts of EpCAM and MUC1 adaptor proteins, and infected SW620 cells. As displayed in Figure 5D, these two adaptor proteins could dramatically enhance the infection efficiency of ADV5 in SW620 cells. The infection efficiency up-regulated by EpCAM adaptor was more remarkable than that by MUC1 adaptor, which could be correlated with the difference of their expression levels in SW620 cells (Figure 5B). The results indicated that the infection efficiency of the complex combining ADV5 and adaptor depended on expression level of a cell surface marker targeted by adaptor. Since EpCAM was

extensively over-expressed in CRC cells, EpCAM adaptor might up-regulate the infection efficiency of ADV5 in the majority of CRC cases.

Furthermore, the functions of engineered proteins were validated *in vivo*. The ADV5 expressing SaCas9 (Additional File 2: Figure S1B) was intratumorally or intravenously injected into nude mice with SW620 cells-derived xenografts (SW620 CDX model), individually or via combination of EpCAM adaptor and protector proteins. According to the expression levels of SaCas9 in tissues collected 48 h after administration, the intratumorally delivered ADV5 was mainly enriched in tumor tissue. The intravenously delivered ADV5 had diverse tissue tropisms, especially towards liver. Adaptor protein significantly enhanced the tumor tropism of ADV5, and reduced the off-target tropisms towards the majority of organs except for colon where EpCAM was also over-expressed (Figure 5E). The addition of protector protein significantly reduced the off-targeting tropisms in a variety of organs including colon, and enhanced the tumor tropism compared with adaptor only (Figure 5E). Therefore, the combination of adaptor and protector could retarget ADV5 to CRC cells over-expressing EpCAM, and reduce its tissue off-targeting *in vivo*. The complex combining ADV5 and the two engineered proteins might be a proper vector to deliver CRISPR system intravenously.

Quadruple-editing of KRAS, MEK1, PIK3CA, and MTOR blocked the progression of KRAS-mutated CRC cells *in vivo*

To evaluate the therapeutic potential of quadruple-editing of MAPK and PI3K pathways mediated by the complex combining ADV5 and engineered proteins, the ADV5 vectors depleting KRAS, MEK1, PIK3CA, and MTOR (KMPM-KO) and non-targeting controls (NT) were pre-incubated with adaptor and protector proteins, and then, were intravenously injected into CDX model of HCT116 (KRAS G13D and PIK3CA H1047R) and PDX model of CRC-PDX01 (KRAS G12V), respectively. The ADV-protein complex (APC) was injected for 2 rounds on Day-0 and Day-12, in which the number of viral particles was 7.0×10^{9} and the amount of protein was 1.0×10^{-7} pmol. The viral distributions in CDX and PDX mice injected with NT and KMPM-KO were checked on Day-2 post-administration (Figure 6A). According to the expression level of SaCas9 in different tissues, NT and KMPM-KO mainly infected the tumor tissues of CDX and PDX mice, indicating the infection specificity of APC. Similar expression level of SaCas9 in the tumor tissues of mice infected with NT and KMPM-KO indicated equal infection efficiencies of these two types of virus (Figure 6B, 6G). The expression level of SaCas9 in the tumor tissues of CRC-PDX01 mice was higher than that in HCT116-CDX mice, which might result from the higher expression level of EpCAM in CRC-PDX01 than that in HCT116 cells (Figure 5B-5C, 6B, 6G). The tumor growth in CDX and PDX mice that received KMPM-KO was significantly blocked compared with those that were given NT (Figure 6C, 6H). Besides, the final tumor volume in CDX and PDX mice that received KMPM-KO was markedly reduced compared with those that were given NT (Figure 6D, 6I). Furthermore, H&E staining of different tissues in CDX and PDX mice showed that the tumor tissues injected with KMPM-KO had a more significant cell necrosis compared with those that received NT (Figure 6E, 6J). These results strongly suggested that quadruple-editing of MAPK and PI3K pathways blocked the progression of KRAS-mutated CRC cells *in vivo.* In addition, no injuries were observed by H&E staining in liver, lung, kidney, and colon of CDX and PDX mice that were

given NT and KMPM-KO (Figure 6E, 6J). No significant difference was noted in body weight of CDX and PDX mice that received NT and KMPM-KO APCs (Figure 6F, 6K). Therefore, the EpCAM-targeting APC could be a specific and safe vector for intravenous delivery of CRISPR system to CRC.

Quadruple-editing blocked MAPK and PI3K pathways in KRAS-mutated CRC cells *in vivo*

The results of T7E1 assay in the tumor tissues of CDX and PDX mice injected with NT and KMPM-KO showed that compared with NT samples, the genomic regions of the four target genes, including KRAS, MEK1, PIK3CA, and MTOR, were all efficiently edited in KMPM-KO samples (Figure 7A, 7D). According to the results of immunohistochemistry (IHC) and Western blotting, the expression levels of the four target genes were significantly down-regulated in KMPM-KO samples compared with those in NT samples (Figure 7B-7C, 7E-7F). The Ki67 staining indicated that the proliferation of tumor cells after quadruple-depletion was notably down-regulated compared with that in control cells (Figure 7B, 7E). Furthermore, the phosphorylation levels of components of MAPK and PI3K pathways, such as ERK, AKT, and S6K, were remarkably down-regulated in KMPM-KO samples compared with those in NT samples (Figure 7C, 7F). The above-mentioned findings indicated that quadruple-editing of the four target genes mediated by EpCAM-targeting APC efficiently blocked MAPK and PI3K pathways in KRAS-mutated CRC cells *in vivo.*

The status of on-target and off-target mutations in tumor tissues induced by quadruple-editing

Whole-exome sequencing (WES) was performed in the tumor tissues of HCT116 CDX mice that received NT and KMPM-KO to detect the mutation status induced by quadruple-editing. The sequencing depth was over 100×. Totally, seven types of on-target deletions were detected at genomic regions of the four target genes (KRAS, MEK1, PIK3CA, and MTOR). The total mutation frequencies of the four target genes were 34.9%, 80%, 40.4%, and 73.3%, respectively (Figure 8A). Among 167 potential off-target loci of these genes predicted by Benchling tool, only one locus of MTOR was detected with a real off-target single-nucleotide variant (SNV) (Chr16, 28603692 C>T), whose mutation frequency was 1.68% (Figure 8B). Furthermore, the total number of variants detected in NT and KMPM-KO samples was almost equal (24420 versus 24539). The number of insertion/deletions (INDELs) and single nucleotide variations (SNVs) detected at different genomic regions was also similar in NT and KMPM-KO samples (Figure 8C-8D). Additionally, the majority of variants detected at different chromosomes were common ones shared by NT and KMPM-KO samples (Figure 8E). These results strongly suggested the minor effect of quadruple-editing on the mutation status of CRC.

Altogether, the quadruple-depletion of KRAS, MEK1, PIK3CA, and MTOR intravenously delivered by the EpCAM-targeting APC blocked MAPK and PI3K pathways and the progression of KRAS-mutated CRC cells with high efficiency and specificity.

Discussion

The present study developed a quadruple-editing system for KRAS, MEK1, PIK3CA, and MTOR based on CRISPR/SaCas9, which could efficiently inhibit MAPK and PI3K pathways and significantly block the

proliferation and invasion of CRC cells with diverse KRAS mutations or oncogenic mutations of KRAS and PIK3CA (Additional File 6: Figure S5). We also constructed two proteins, an adaptor and a protector, to form a complex with ADV5 and facilitate the intravenous delivery of CRISPR system to CRC cells over-expressing EpCAM. The quadruple-editing of MAPK and PI3K pathways delivered by the APC blocked the tumor progression of KRAS-mutated CDX and PDX models with high efficacy and specificity. As EpCAM showed to have high expression levels in CRC cases [24], our quadruple-editing system could cover the majority of KRAS-mutated CRC cells, highlighting its clinical significance for CRC treatment.

Although recent development of inhibitors against KRAS G12C and MEK had shed light on the treatment of a number of KRAS-mutated CRC cases, the diversity of KRAS variants and aberrant activation of PI3K pathway are still critical bottlenecks for the therapy of the majority of CRC patients. There are over ten types of oncogenic mutations in codon 12/13 of KRAS, such as G12D/V/C/S/A/R and G13D/C, and the majority of them have no promising inhibitors [25]. PI3K pathway could be activated by RTKs, compromising the inhibitory effect of MEK. The overlapping toxicities limit the clinical significance of combined therapies with inhibitors of MAPK and PI3K pathways [7, 8]. The proposed quadruple-editing system could simultaneously deplete four key components of MAPK and PI3K pathways, including KRAS, MEK1, PIK3CA, and MTOR, and perfectly solved the issues of diverse KRAS mutations and compensated PI3K activation under MAPK suppression. According to the results of WES analysis of tumor tissues with gene editing, quadruple-depletion rarely induced off-target mutation, and showed to have a minor influence on the mutation status of CRC. No injury was detected in the vital organs of mice with gene editing, including liver, lung, kidney, and colon, on the basis of the results of H&E staining. These results strongly demonstrated the high specificity and low toxicity of quadruple-editing system. However, it is highly essential to investigate the individual and combined effects of available inhibitors and quadruple-editing vector of MAPK and PI3K pathways in the future study to validate the clinical application of CRISPR system in CRC treatment.

The four genes, KRAS, MEK, PIK3CA and MTOR, are the most common therapeutic targets for CRC treatment at present. KRAS mutation occurs in nearly 50% CRC patients, PIK3CA mutation is just second only to KRAS, approximately 18% in CRC [26, 27]. Considering both of them are activating mutations and the crosstalk between MAPK and PI3K pathways [28], knockout of KRAS and PIK3CA was essential in KRAS mutated CRC. Moreover, targeting KRAS and PIK3CA together with their down-stream intermediates MEK and MTOR could more effectively inhibit the activation of those pathways. For instance, targeting MTOR could inhibit the activation of PI3K pathway induced by PTEN and AKT mutations. Targeting MEK could inhibit the activation of MAPK pathway induced by BRAF mutation. Many studies have demonstrated that the effect of dual inhibition of two molecules was better than inhibition of one molecule alone in MAPK or PI3K pathway. Taken MAPK pathway for example, several clinical trials proved that the combination treatment of BRAF and MEK inhibitors was more efficient than the application of BRAF inhibitor alone in BRAF mutant melanoma and non-small cell lung cancer [29-32]. Patients received combined regimens including BRAF and MEK inhibitors presented a prolonged overall survival than the control group in a BRAF V600E mutated CRC clinical trial [33]. For PI3K pathway, dual inhibitors of PI3K/MTOR displayed a stronger effect than MTOR inhibitor alone in not only hematological

tumors but also solid tumors [34-36]. Furthermore, based on our data, simultaneously depleting KRAS/MEK1 and PIK3CA/MTOR respectively inhibited the signaling of MAPK and PI3K, more significantly than individual depletions, revealed by the extents of down-regulation of phosphorylated ERK and S6K (Figure 2C-2D, 3C-3D). Depleting the signaling intermediates together provided better anti-tumor effects than depleting KRAS and PIK3CA only (Figure 2F-2G, 3F-3G). Therefore, targeting two genes in one pathway is a better strategy than single targeting.

Here, we constructed an APC through combining ADV with an adaptor and a protector to overcome major challenges limiting systemic delivery of ADV. This two-protein construction efficiently retargeted ADV from its common receptor (CXADR) to EpCAM, a membrane protein over-expressing in CRC cells, and significantly reduced the tissue off-targeting of ADV, especially the liver tropism with over 10000 folds, which was better than the performance of some polymers such as polyethylene glycol (PEG) reported previously [20]. The proteomic studies had revealed protein markers in different types of cancer, including gastric cancer and pancreatic cancer. The EpCAM-targeting module of an adaptor protein was found exchangeable and could be replaced with scFv against membrane markers in gastric and pancreatic cancer cells, e.g. proteins of MUCIN family [37, 38], accordingly forming specific APC for gene therapies in these types of cancer.

Conclusions

In summary, CRISPR-mediated quadruple-depletion of KRAS, MEK1, PIK3CA, and MTOR intravenously delivered by ADV-protein complex could be a promising therapeutic option for KRAS-mutated CRC cells. In the future, the adaptor and sgRNA libraries will be established, and the genome editing therapy will have extensive applications in different types of cancer.

Declarations

Ethics approval and consent to participate

Written informed consent was obtained from all patients prior to commencing the study. Study protocols were approved by the Ethics Committee of Peking University Cancer Hospital & Institute (Approval No. 2015KT71) and based on the ethical principles for medical research involving human subjects of the Helsinki Declaration. Animal experiments were approved by the Animal Ethics Committee of Peking University Cancer Hospital & Institute, and performed in full compliance with the Experimental Animal Management Ordinance produced by the Peking University Cancer Hospital & Institute.

Consent for publication

Not applicable.

Availability of data and materials

The sequencing data reported in this study are available in the CNGB Nucleotide Sequence Archive. https://db.cngb.org/cnsa. Accession number CNP0000324.

Competing interests

The authors declare that they have no competing interests.

Funding

This work was supported by the grants from National Natural Science Foundation of China (No. 82073357, No. 81872022, No. 81672439, No. 81903159, and No. 81972678), Capital's Funds for Health Improvement and Research (CFH 2018-2-2153), Beijing Natural Science Foundation (No. 7172042, and No. 7192037), Science Foundation of Peking University Cancer Hospital (No. 2017-14), Science, Technology and Innovation Commission of Shenzhen Municipality (No. JCYJ20170817145218948), and Guangdong Provincial Key Laboratory of Genome Read and Write (No. 2017B030301011).

Authors' contributions

1. Kang, J. Li, and XQ. Su conceived and designed the study. ZZ. Wang, B. Kang and QQ. Gao performed all the in vitro experiments. ZZ. Wang, JH. Yu, YC. Fan and JB. Di performed the animal experiments in vivo. L. Huang, F. Gao, and D. Wang provided support with experimental techniques. HX. Sun, BH. Jiang, and Y. Gu collected and analyzed data, B. Kang, ZZ. Wang, and QQ. Gao prepared the manuscript. J. Li and XQ. Su reviewed and revised the manuscript. All authors read and approved the final manuscript.

Acknowledgements

Not applicable.

Abbreviations

CRISPR: clustered regularly interspaced short palindromic repeats; CRC: colorectal cancer; MAPK: mitogen-activated protein kinase; PI3K: phosphatidylinositol 3-kinase; MTOR: mammalian target of rapamycin; ADV5: serotype 5 of adenovirus; APC: ADV-protein complex; EpCAM: epithelial cell adhesion molecule; AKT: protein kinase B; DSB: double-strand break; scFv: single-chain variable fragment; HER2: human epidermal growth factor receptor 2; sgRNA: single guide RNA; RT-qPCR: quantitative reverse transcription-polymerase chain reaction; IC50: half maximal inhibitory concentration; PDX: patient-derived xenograft; CXADR: coxsackievirus and adenovirus receptor; ECXADR: ectodomain of ADV receptor CXADR; MUC1: Mucin 1, cell surface associated; GFP: green fluorescent protein; FACS: fluorescence-activated cell sorting; i.t.: intratumoral; i.v.: intravenous; NT: non-targeting; IHC: immunohistochemistry; WES: whole-exome sequencing; INDEL: insertion/deletion; SNV: single nucleotide variation; PEG: polyethylene glycol; RPMI: Roswell park memorial institute; NOD-SCID: non-obese diabetic severe combined immunodeficient; DMEM: Dulbecco's modified Eagle's medium; FBS: fetal bovine serum; SDS-

PAGE: sodium dodecyl sulfate-polyacrylamide gel electrophoresis; PVDF: polyvinylidene fluoride; BSA: bovine serum albumin; HRP: horseradish peroxidase; H&E: hematoxylin and eosin; PBS: phosphate-buffered saline; ANOVA: two-way analysis of variance.

References

1. Bray F, Ferlay J, Soerjomataram I, Siegel RL, Torre LA, Jemal A. Global cancer statistics 2018: GLOBOCAN estimates of incidence and mortality worldwide for 36 cancers in 185 countries. CA Cancer J Clin. 2018;68:394-424.
2. Markowitz SD, Bertagnolli MM. Molecular origins of cancer: Molecular basis of colorectal cancer. N Engl J Med. 2009;361:2449-60.
3. Liu P, Wang Y, Li X. Targeting the untargetable KRAS in cancer therapy. Acta Pharm Sin B. 2019;9:871-9.
4. Canon J, Rex K, Saiki AY, Mohr C, Cooke K, Bagal D, et al. The clinical KRAS(G12C) inhibitor AMG 510 drives anti-tumour immunity. Nature. 2019;575:217-23.
5. Ebi H, Corcoran RB, Singh A, Chen Z, Song Y, Lifshits E, et al. Receptor tyrosine kinases exert dominant control over PI3K signaling in human KRAS mutant colorectal cancers. J Clin Invest. 2011;121:4311-21.
6. Vitiello PP, Cardone C, Martini G, Ciardiello D, Belli V, Matrone N, et al. Receptor tyrosine kinase-dependent PI3K activation is an escape mechanism to vertical suppression of the EGFR/RAS/MAPK pathway in KRAS-mutated human colorectal cancer cell lines. J Exp Clin Cancer Res. 2019;38:41.
7. Schram AM, Gandhi L, Mita MM, Damstrup L, Campana F, Hidalgo M, et al. A phase Ib dose-escalation and expansion study of the oral MEK inhibitor pimasertib and PI3K/MTOR inhibitor voxtalisib in patients with advanced solid tumours. Br J Cancer. 2018;119:1471-6.
8. Do K, Speranza G, Bishop R, Khin S, Rubinstein L, Kinders RJ, et al. Biomarker-driven phase 2 study of MK-2206 and selumetinib (AZD6244, ARRY-142886) in patients with colorectal cancer. Invest New Drugs. 2015;33:720-8.
9. Zhang F, Wen Y, Guo X. CRISPR/Cas9 for genome editing: progress, implications and challenges. Hum Mol Genet. 2014;23:R40-6.
10. Cong L, Ran FA, Cox D, Lin S, Barretto R, Habib N, et al. Multiplex genome engineering using CRISPR/Cas systems. Science. 2013;339:819-23.
11. Kabadi AM, Ousterout DG, Hilton IB, Gersbach CA. Multiplex CRISPR/Cas9-based genome engineering from a single lentiviral vector. Nucleic Acids Res. 2014;42:e147.
12. Stadtmauer EA, Fraietta JA, Davis MM, Cohen AD, Weber KL, Lancaster E, et al. CRISPR-engineered T cells in patients with refractory cancer. Science. 2020;367: eaba7365
13. Ren J, Liu X, Fang C, Jiang S, June CH, Zhao Y. Multiplex Genome Editing to Generate Universal CAR T Cells Resistant to PD1 Inhibition. Clin Cancer Res. 2017;23:2255-66.

14. Ran FA, Cong L, Yan WX, Scott DA, Gootenberg JS, Kriz AJ, et al. In vivo genome editing using Staphylococcus aureus Cas9. Nature. 2015;520:186-91.
15. Maeder ML, Stefanidakis M, Wilson CJ, Baral R, Barrera LA, Bounoutas GS, et al. Development of a gene-editing approach to restore vision loss in Leber congenital amaurosis type 10. Nat Med. 2019;25:229-33.
16. Lee W, Lee JH, Jun S, Lee JH, Bang D. Selective targeting of KRAS oncogenic alleles by CRISPR/Cas9 inhibits proliferation of cancer cells. Sci Rep. 2018;8:11879.
17. Gao Q, Ouyang W, Kang B, Han X, Xiong Y, Ding R, et al. Selective targeting of the oncogenic KRAS G12S mutant allele by CRISPR/Cas9 induces efficient tumor regression. Theranostics. 2020;10:5137-53.
18. Yoon AR, Hong J, Kim SW, Yun CO. Redirecting adenovirus tropism by genetic, chemical, and mechanical modification of the adenovirus surface for cancer gene therapy. Expert Opin Drug Deliv. 2016;13:843-58.
19. Kashentseva EA, Seki T, Curiel DT, Dmitriev IP. Adenovirus targeting to c-erbB-2 oncoprotein by single-chain antibody fused to trimeric form of adenovirus receptor ectodomain. Cancer Res. 2002;62:609-16.
20. Schmid M, Ernst P, Honegger A, Suomalainen M, Zimmermann M, Braun L, et al. Adenoviral vector with shield and adapter increases tumor specificity and escapes liver and immune control. Nat Commun. 2018;9:450.
21. Cancer Genome Atlas N. Comprehensive molecular characterization of human colon and rectal cancer. Nature. 2012;487:330-7.
22. Khare R, Chen CY, Weaver EA, Barry MA. Advances and future challenges in adenoviral vector pharmacology and targeting. Curr Gene Ther. 2011;11:241-58.
23. Lugli A, Iezzi G, Hostettler I, Muraro MG, Mele V, Tornillo L, et al. Prognostic impact of the expression of putative cancer stem cell markers CD133, CD166, CD44s, EpCAM, and ALDH1 in colorectal cancer. Br J Cancer. 2010;103:382-90.
24. Belov L, Zhou J, Christopherson RI. Cell surface markers in colorectal cancer prognosis. Int J Mol Sci. 2010;12:78-113.
25. Lim B, Mun J, Kim JH, Kim CW, Roh SA, Cho DH, et al. Genome-wide mutation profiles of colorectal tumors and associated liver metastases at the exome and transcriptome levels. Oncotarget. 2015;6:22179-90.
26. Albertini AF, Raoux D, Neumann F, Rossat S, Tabet F, Pedeutour F, et al. [Detection of RAS genes mutation using the Cobas((R)) method in a private laboratory of pathology: Medical and economical study in comparison to a public platform of molecular biology of cancer]. Bull Cancer. 2017;104:662-74.
27. Yaeger R, Chatila WK, Lipsyc MD, Hechtman JF, Cercek A, Sanchez-Vega F, et al. Clinical Sequencing Defines the Genomic Landscape of Metastatic Colorectal Cancer. Cancer Cell. 2018;33:125-36 e123.

28. Carracedo A, Ma L, Teruya-Feldstein J, Rojo F, Salmena L, Alimonti A, et al. Inhibition of mTORC1 leads to MAPK pathway activation through a PI3K-dependent feedback loop in human cancer. J Clin Invest. 2008;118:3065-74.
29. Long GV, Stroyakovskiy D, Gogas H, Levchenko E, de Braud F, Larkin J, et al. Combined BRAF and MEK inhibition versus BRAF inhibition alone in melanoma. N Engl J Med. 2014;371:1877-88.
30. Dummer R, Ascierto PA, Gogas HJ, Arance A, Mandala M, Liszkay G, et al. Encorafenib plus binimetinib versus vemurafenib or encorafenib in patients with BRAF-mutant melanoma (COLUMBUS): a multicentre, open-label, randomised phase 3 trial. Lancet Oncol. 2018;19:603-15.
31. Planchard D, Besse B, Groen HJM, Souquet PJ, Quoix E, Baik CS, et al. Dabrafenib plus trametinib in patients with previously treated BRAF(V600E)-mutant metastatic non-small cell lung cancer: an open-label, multicentre phase 2 trial. Lancet Oncol. 2016;17:984-93.
32. Johnson DB, Flaherty KT, Weber JS, Infante JR, Kim KB, Kefford RF, et al. Combined BRAF (Dabrafenib) and MEK inhibition (Trametinib) in patients with BRAFV600-mutant melanoma experiencing progression with single-agent BRAF inhibitor. J Clin Oncol. 2014;32:3697-704.
33. Kopetz S, Grothey A, Yaeger R, Van Cutsem E, Desai J, Yoshino T, et al. Encorafenib, Binimetinib, and Cetuximab in BRAF V600E-Mutated Colorectal Cancer. N Engl J Med. 2019;381:1632-43.
34. Mazzoletti M, Bortolin F, Brunelli L, Pastorelli R, Di Giandomenico S, Erba E, et al. Combination of PI3K/mTOR inhibitors: antitumor activity and molecular correlates. Cancer Res. 2011;71:4573-84.
35. Bresin A, Cristofoletti C, Caprini E, Cantonetti M, Monopoli A, Russo G, et al. Preclinical Evidence for Targeting PI3K/mTOR Signaling with Dual-Inhibitors as a Therapeutic Strategy against Cutaneous T-Cell Lymphoma. J Invest Dermatol. 2020;140:1045-53 e1046.
36. Cho DC, Cohen MB, Panka DJ, Collins M, Ghebremichael M, Atkins MB, et al. The efficacy of the novel dual PI3-kinase/mTOR inhibitor NVP-BEZ235 compared with rapamycin in renal cell carcinoma. Clin Cancer Res. 2010;16:3628-38.
37. Ge S, Xia X, Ding C, Zhen B, Zhou Q, Feng J, et al. A proteomic landscape of diffuse-type gastric cancer. Nat Commun. 2018;9:1012.
38. Pan S, Chen R, Tamura Y, Crispin DA, Lai LA, May DH, et al. Quantitative glycoproteomics analysis reveals changes in N-glycosylation level associated with pancreatic ductal adenocarcinoma. J Proteome Res. 2014;13:1293-6.

Figures

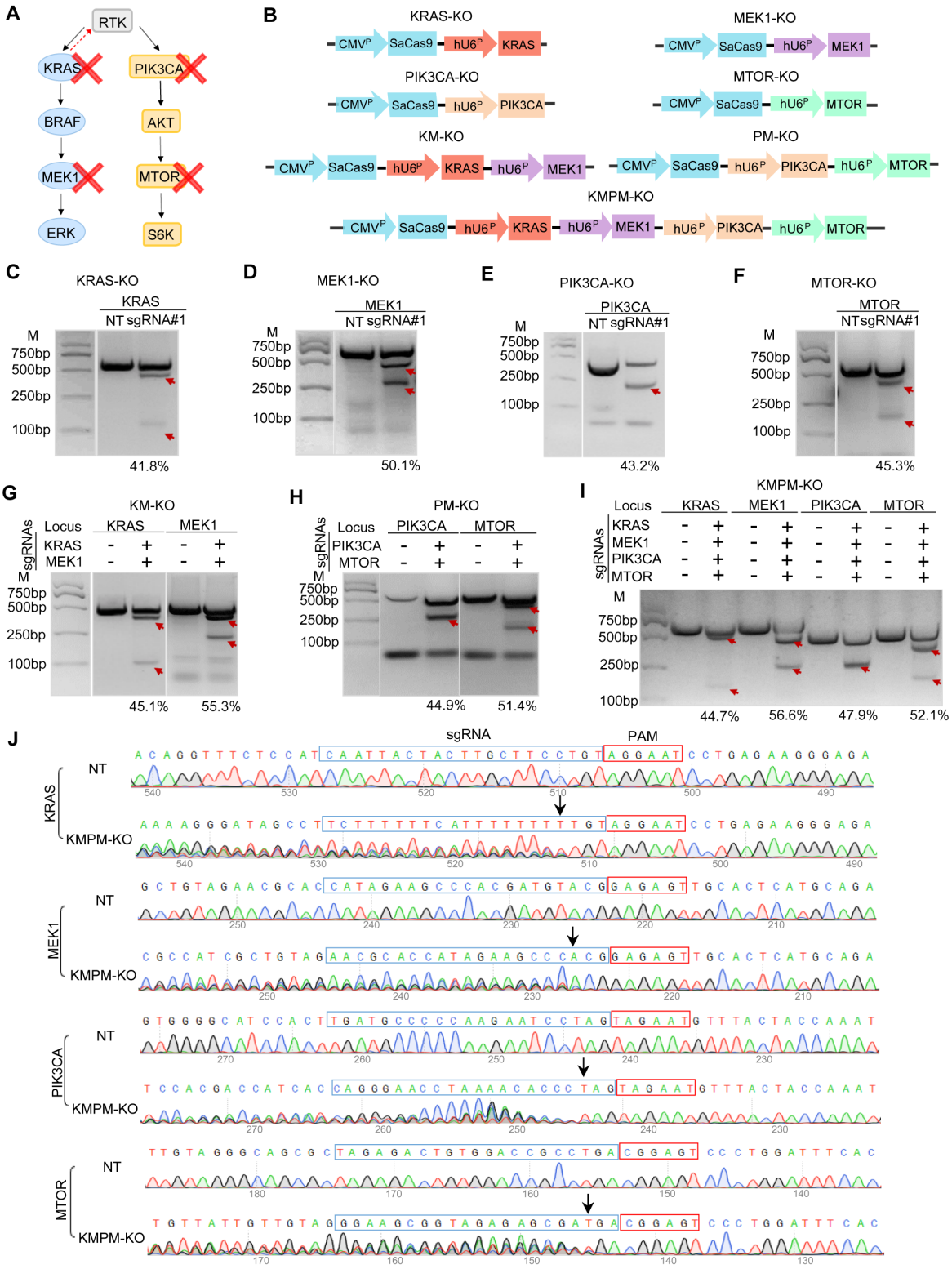

Figure 1

Constructing single- and multiple-editing vectors targeting MAPK and PI3K pathways. (A). A diagram of components in MAPK and PI3K pathways. The red crossing mark indicated the editing targets. And the red and dotted arrow indicated the compensated activation of RTK under MAPK suppression. (B). A diagram of single- and multiple-editing vectors of KRAS, MEK1, PIK3CA and MTOR. P indicated promoter, and sgRNA cassettes were symbolized by corresponding gene names. KM-KO, PM-KO, and KMPM-KO

respectively indicated the double- and quadruple- editing of MAPK and PI3K pathways. (C-I). Editing effects of single- and multiple-editing vectors in 293T cells. The effects of single- and multiple-editing vectors were respectively detected by T7E1 assays. NT indicated non-targeting control. The editing efficiencies were listed below the graphs. The red arrows denoted the cleavage products of T7E1 assay. (J). Sanger sequencing of target genomic regions of quadruple-editing in 293T cells. The sgRNA and PAM sequences of the four target genes were respectively labeled in blue and red boxes. The arrow indicated the start site of on-target mutation.

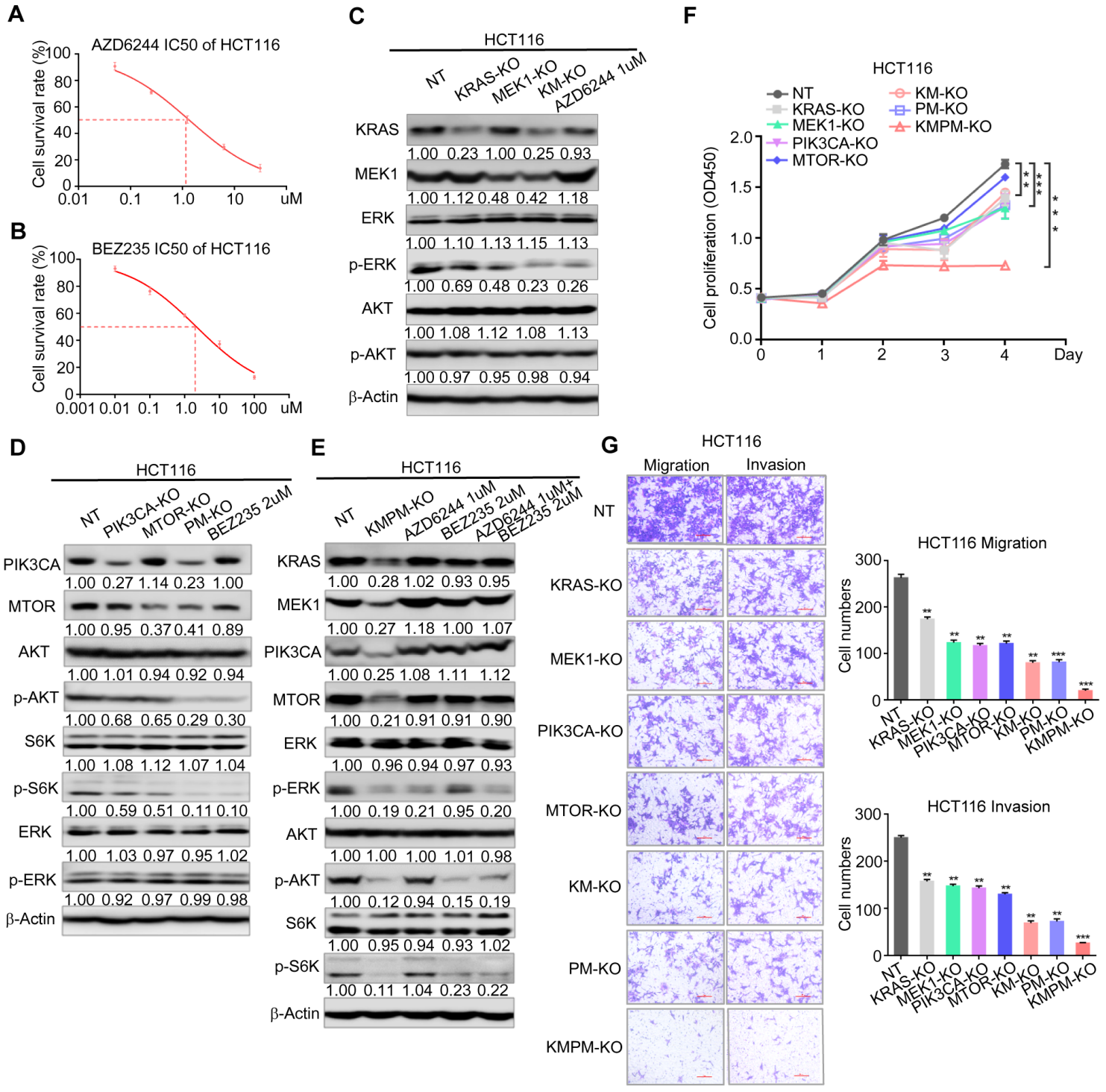

Figure 2

Quadruple-editing inhibited MAPK and PI3K pathways in CRC cells with double mutations of KRAS and PIK3CA. (A-B) Survival rates of HCT116 cells treated with various concentrations of MEK inhibitor AZD6244 and PI3K/MTOR inhibitor BEZ235. The IC50 values of AZD6244 and BEZ235 were respectively indicated by dotted line in (A) and (B). (C-E). Western blotting of MAPK and PI3K signaling in HCT116 cells with single- and multiple-editing of KRAS, MEK1, PIK3CA and MTOR, and with the treatments of AZD6244 and BEZ235. NT indicated non-targeting control. The quantification of densitometry normalized to β-Actin was presented below the blotting results. (F). Proliferation of HCT116 cells with single- and multiple-editing of the four targets. The results were average of three replicates. The statistical analysis was two-way ANOVA. The significances were respectively referring NT:KM-KO, NT:PM-KO, and NT:KMPM-KO from left to right. ** $0.001 \leq P < 0.01$, *** $P < 0.001$. (G). Migration and invasion of HCT116 cells with single- and multiple-editing of the four targets. The results were average of three replicates. The numbers of migrated and invaded cells were summarized beside the graphs. ** $0.001 \leq P < 0.01$, *** $P < 0.001$.

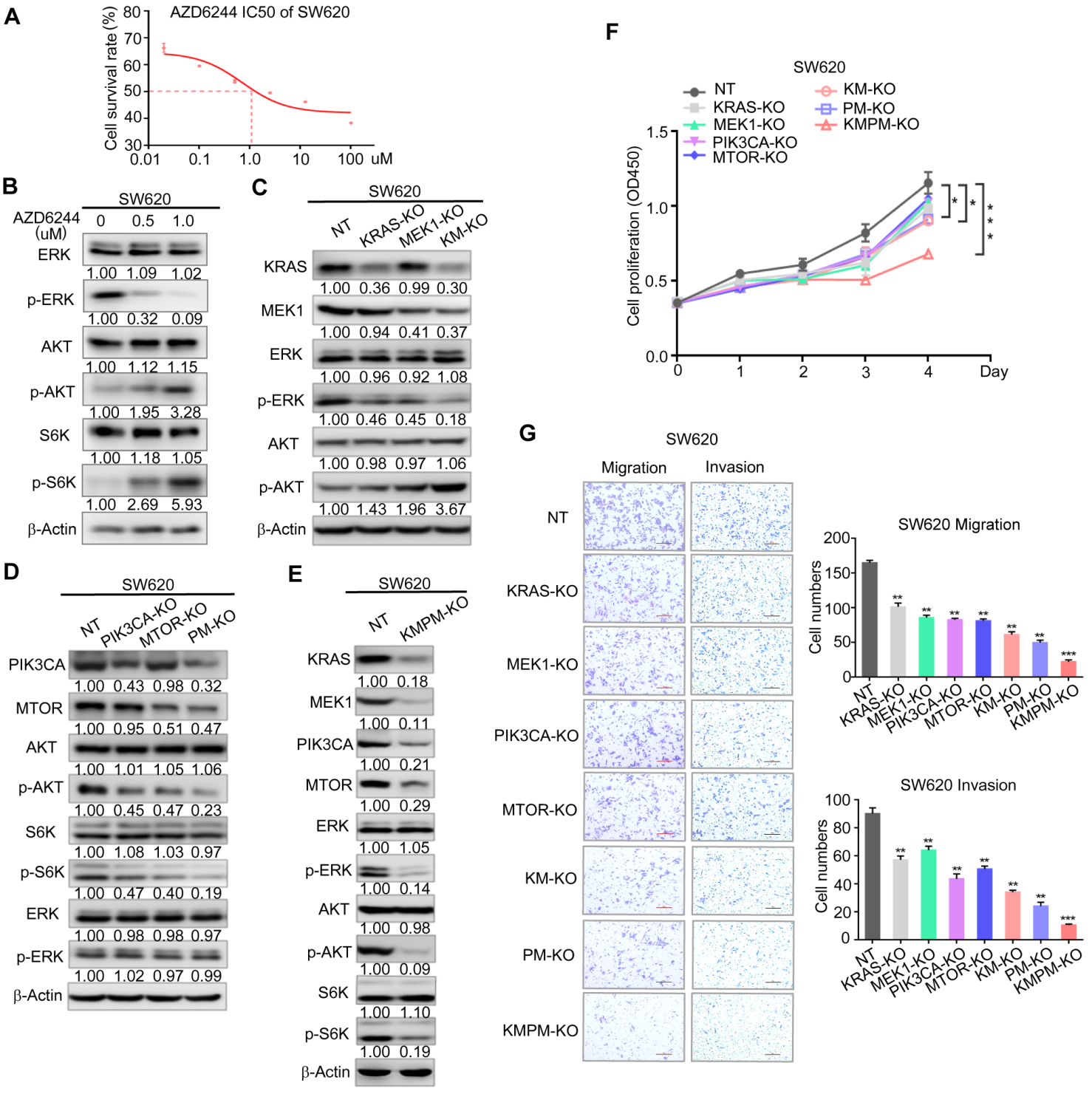

Figure 3

Quadruple-editing inhibited MAPK and PI3K pathways in KRAS-mutated CRC cells with compensated activation of PI3K. (A). Survival rates of SW620 cells treated with various concentrations of MEK inhibitor AZD6244. The IC50 value of AZD6244 was indicated by dotted line. (B). Western blotting of MAPK and PI3K signaling in SW620 cells treated with different concentrations of AZD6244. The blotting densitometry of phosphorylated proteins were normalized to that of β-Actin, and presented below the blotting results. (C-E). Western blotting of MAPK and PI3K signaling in SW620 cells with single- and

multiple-editing of KRAS, MEK1, PIK3CA and MTOR. NT indicated non-targeting control. The blotting densitometry of editing targets and signaling proteins were normalized to that of β-Actin, and presented below the blotting results. (F). Proliferation of SW620 cells with single- and multiple-editing of the four targets. The results were average of three replicates. The statistical analysis was two-way ANOVA. The significances were respectively referring NT:KM-KO, NT:PM-KO, and NT:KMPM-KO from left to right. * $0.01 \leq P < 0.05$, *** $P < 0.001$. (G). Migration and invasion of SW620 cells with single- and multiple-editing of the four targets. The results were average of three replicates. The numbers of migrated and invaded cells were summarized beside the graphs. ** $0.001 \leq P < 0.01$, *** $P < 0.001$.

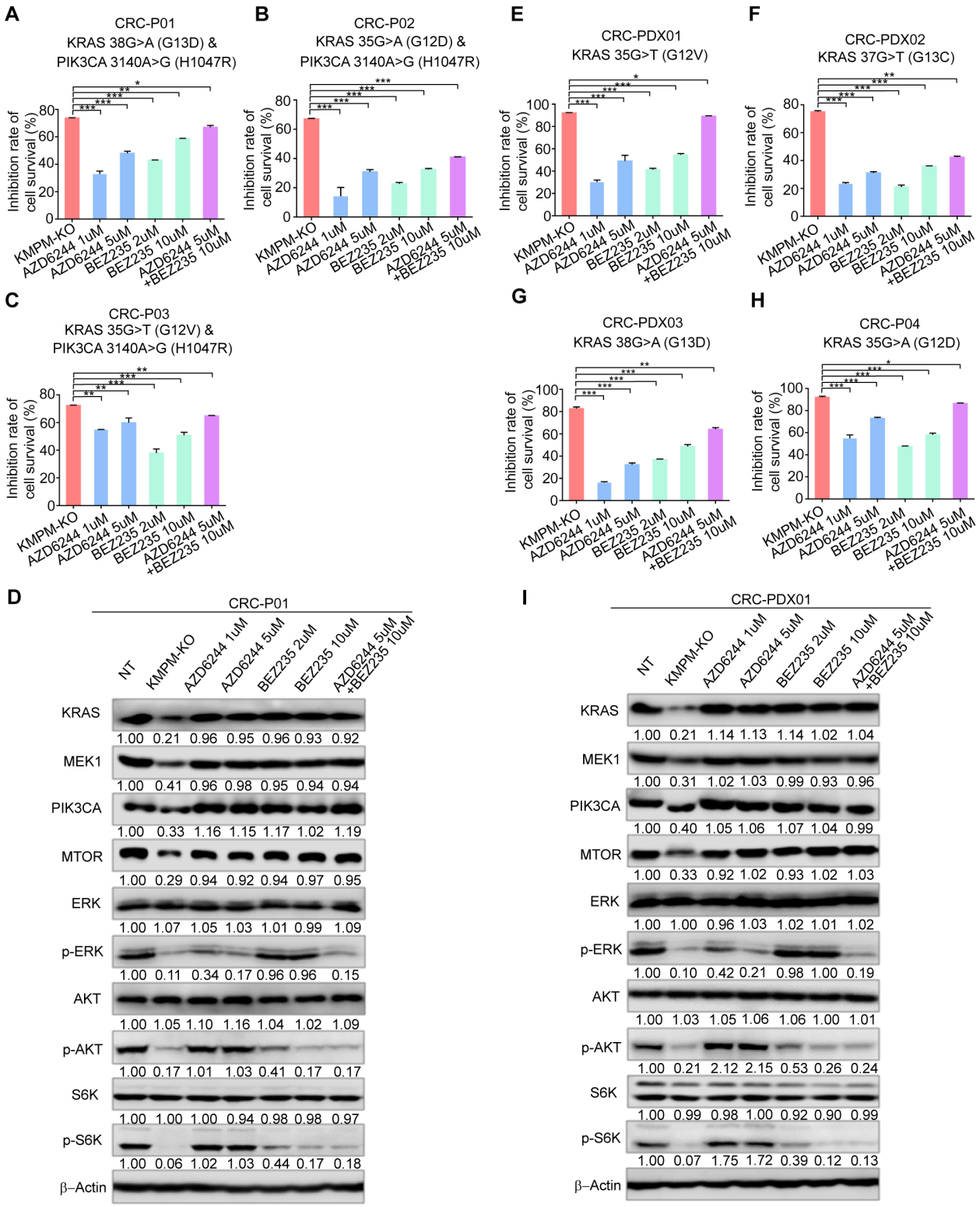

Figure 4

Quadruple-editing inhibited the survival of primary CRC cells with diverse variations of KRAS and PIK3CA. (A-C, E-H). Survival inhibition of primary CRC cells with quadruple-depletion and treatments of MEK and PI3K/MTOR inhibitors. The inhibition rates of cell survival were calculated according to the formula, (1-viability of treated cells/viability of untreated control cells)×100, and were the averages of replicated experiments. The inhibitors of MEK and PI3K/MTOR were respectively AZD6244 and BEZ235. The

mutation status of KRAS and PIK3CA of primary CRC cells were listed above each histogram. (D, I). Western blotting of MAPK and PI3K signaling in primary tumor cells with quadruple-editing of KRAS, MEK1, PIK3CA and MTOR, and with the treatments of AZD6244 and BEZ235. NT indicated non-targeting control. The quantification of densitometry normalized to β-Actin was presented below the blotting results. The primary tumor cells in (D) and (I) were respectively CRC-P01 and CRC-PDX01.

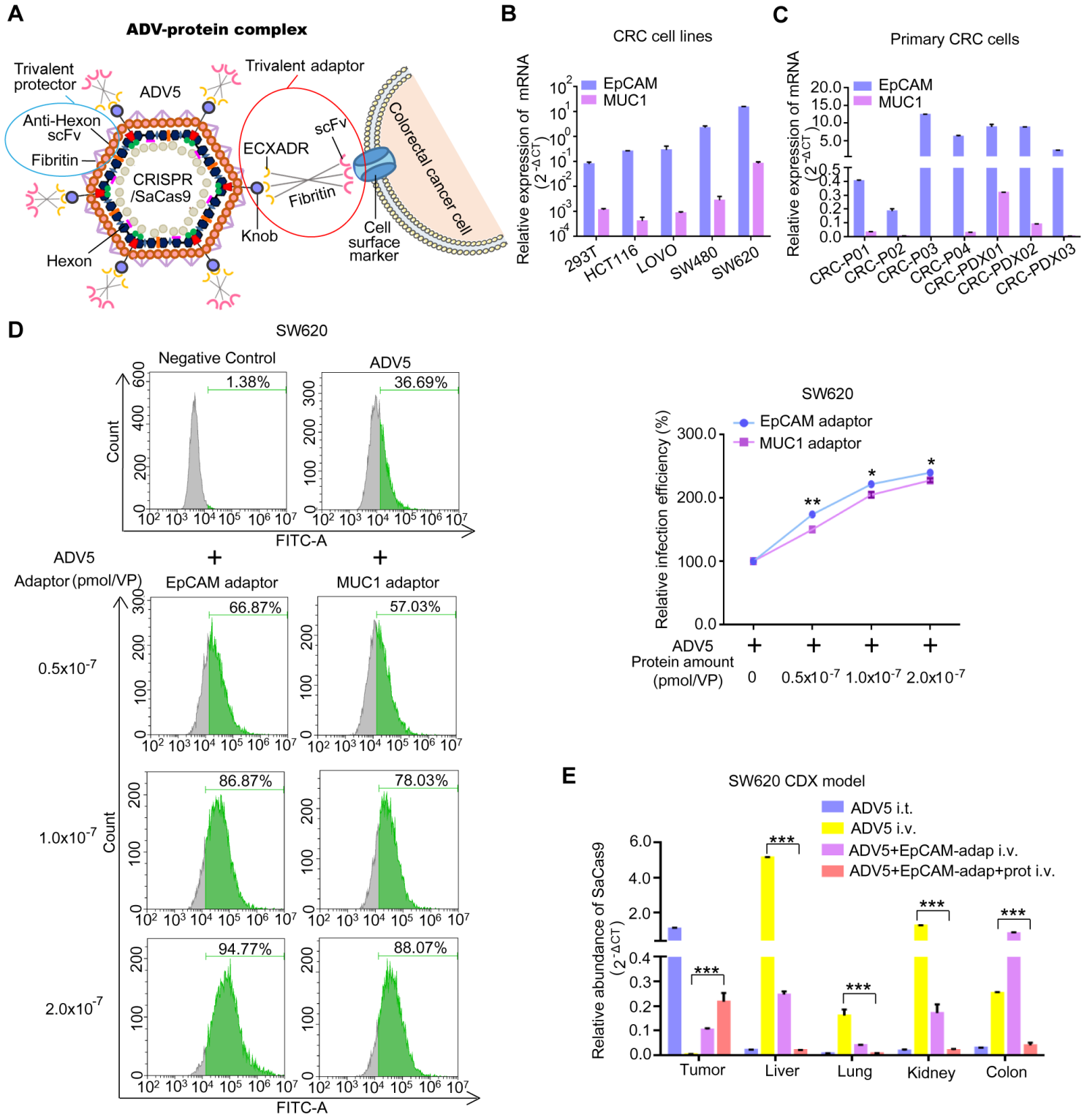

Figure 5

The complex combining ADV5 and engineered proteins intravenously delivered CRISPR system to CRC with high efficiency and specificity. (A). A diagram of ADV-protein complex delivering CRISPR system. The ADV-protein complex (APC) was composed of ADV5 virus and two engineered proteins, an adaptor and a protector. The adaptor protein was composed of the ectodomain of ADV receptor on cell surface CXADR (ECXADR), a phage T4 fibritin polypeptide and a humanized scFv against certain cell surface marker. This adaptor bound to knob protein of ADV5 fiber and retargeted the virus to CRC cells expressing surface marker. The protector protein was composed of a humanized scFv against hexon protein of ADV5 and a phage T4 fibritin polypeptide. This protector covered ADV5 surface and reduced its non-specific tissue tropism. The fibritin linkers trimerized to form the trivalent adaptor and protector proteins. (B-C). Expression levels of EpCAM and MUC1 in CRC cell lines (B) and primary tumor cells (C). (D). Infection efficiencies of ADV5 to SW620 cells combining with various amounts of adaptor proteins of EpCAM and MUC1. The relative infection efficiencies were calculated through comparing the GFP-positive ratios of SW620 cells infected with ADV-protein complex with those infected with ADV individually. The results were average of two replicates. The representative FACS results were presented on the left. * $0.01 \leq P$ 0.05, ** $0.001 \leq P$ 0.01. (E). Virus distribution in a mouse model with SW620 derived xenograft (SW620 CDX) administrated with ADV5 or ADV-protein complex through intratumoral (i.t.) or intravenous (i.v.) method. The different tissue samples were collected 48 h after ADV delivery. The distribution of ADV was indicated by the relative expression of SaCas9. The results were average of two replicates. *** P 0.001.

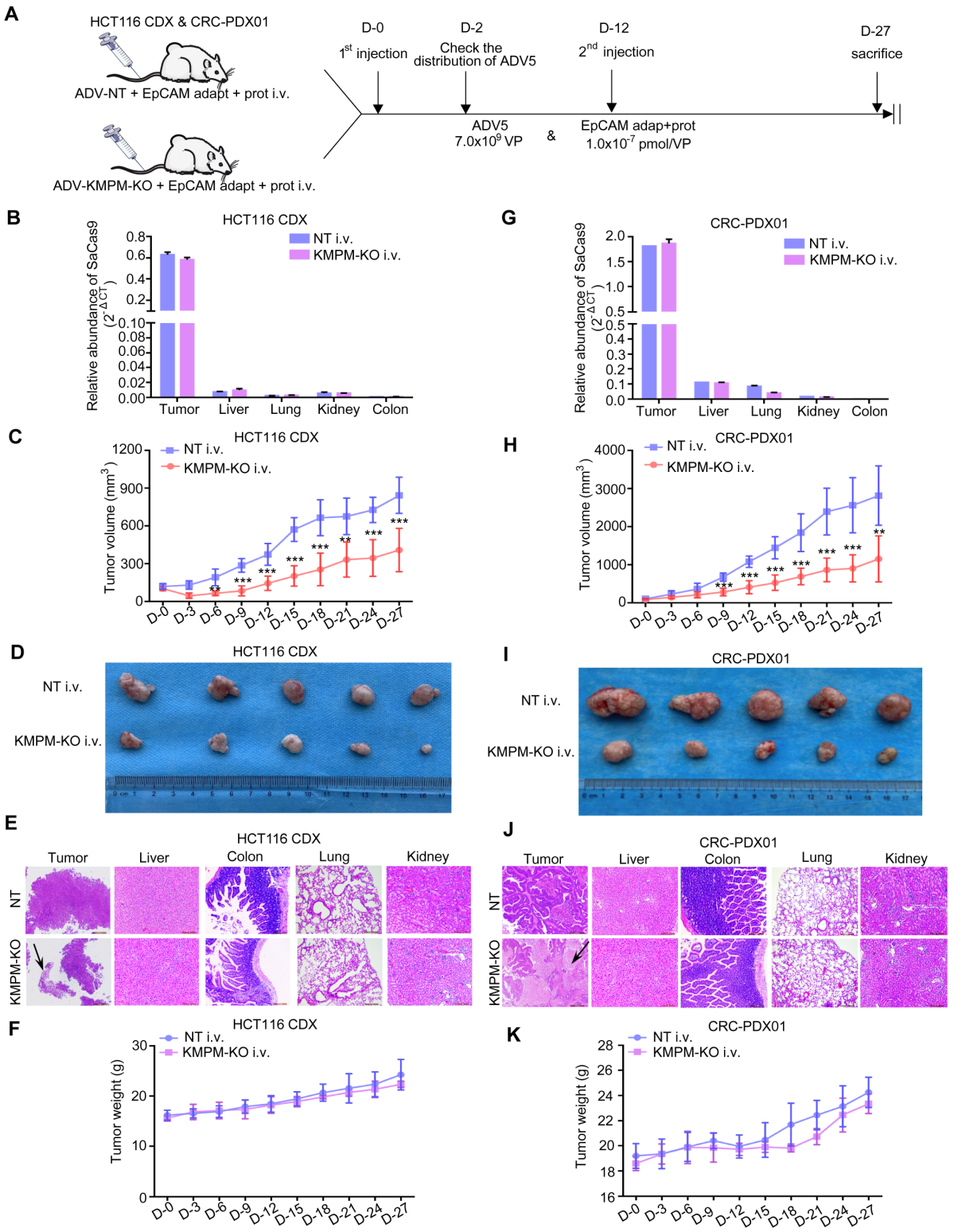

Figure 6

Quadruple-editing of KRAS, MEK1, PIK3CA and MTOR blocked the progression of KRAS-mutated CRC in vivo (A). A diagram of intravenous administration of ADV-protein complex with quadruple-editing in HCT116 CDX and CRC-PDX01 PDX mouse models. ADV5 vector was pre-incubated with the adaptor and the protector proteins to form ADV-protein complex. The APC was injected for 2 rounds at Day-0 and Day-12 with the number of ADV5 viral particles of 7.0×109 and the protein concentration of 1.0×10-7 pmol.

The virus distributions in mice were checked at Day-2 after administration. (B,G). ADV5 distributions in CDX (B) and PDX (G) mice intravenously administrated with ADV-protein complex of quadruple-editing (KMPM-KO) and non-target control (NT). The different tissue samples were collected 48 h after virus delivery. The distribution of ADV5 was indicated by the relative expression of SaCas9, revealed by RT-qPCR. The results were average of two replicates. (C,H). Tumor growth curves of CDX (C) and PDX (H) mice with quadruple-depletion. The number of mice was respectively five for CDX or PDX models administrated with APC of NT or KMPM-KO. ** 0.001≤P□0.01, *** P□0.001. (D,I). Tumor tissues collected from CDX (D) and PDX (I) mice with quadruple-depletion. The tumors were collected at the final observation point (Day-27). The number of tumors was respectively five for CDX or PDX mice administrated with APC of NT or KMPM-KO. (E,J). H&E staining on various tissues of CDX (E) and PDX (J) mice with quadruple-depletion. The tissues were collected at the final observation point (Day-27). The arrow indicated the cell necrosis in tumor tissue. The brown scale bar indicated 200 □M. (F,K). The body weights of CDX (F) and PDX (K) mice with quadruple-depletion.

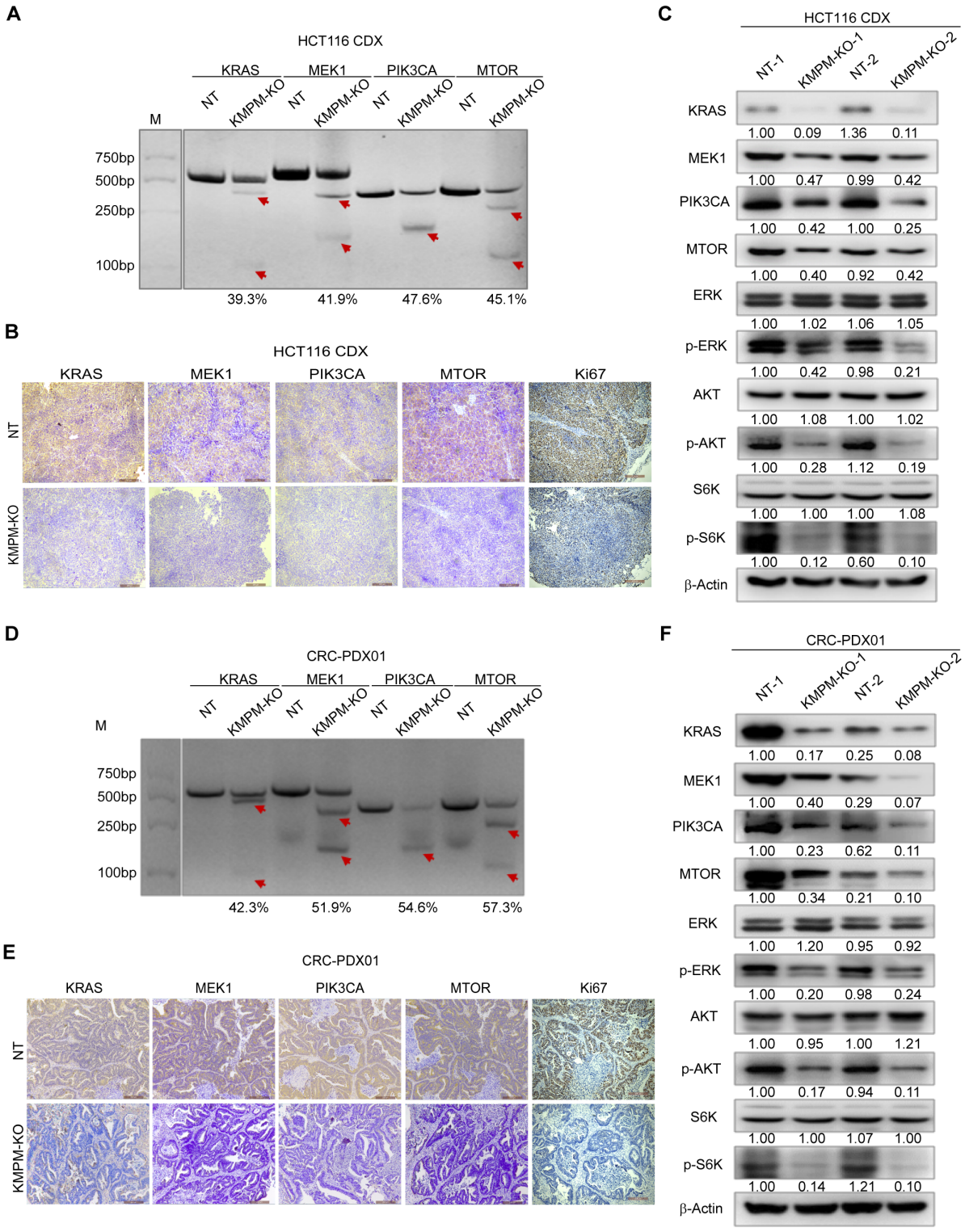

Figure 7

Quadruple-editing blocked MAPK and PI3K signaling in KRAS-mutated CRC in vivo (A,D). T7E1 assays to detect the editing efficiencies of the four target genes in tumor tissues of HCT116 CDX (A) and CRC-PDX01 (D) mice. The tumor samples were collected at the final observation point (Day-27). The editing efficiency was listed below the graph. The red arrows denoted the cleavage products of T7E1 assay. (B,E). IHC assays to detect the depleting effects of the four target proteins and Ki67 levels in tumor tissues of

CDX (B) and PDX (E) mice. The tumor samples were collected at the final observation point (Day-27). The brown scale bar indicated 200 □m. The intensities of brown color in tumor cells were indicators of expression levels of corresponding proteins. (C,F). Western blotting assays to detect the inhibiting effects of MAPK and PI3K pathways in tumor tissues of CDX (C) and PDX (F) mice. The tumor samples were collected at the final observation point (Day-27). The blotting densitometry of targets and phosphorylated proteins were normalized to that of □-Actin, and presented below the blotting results.

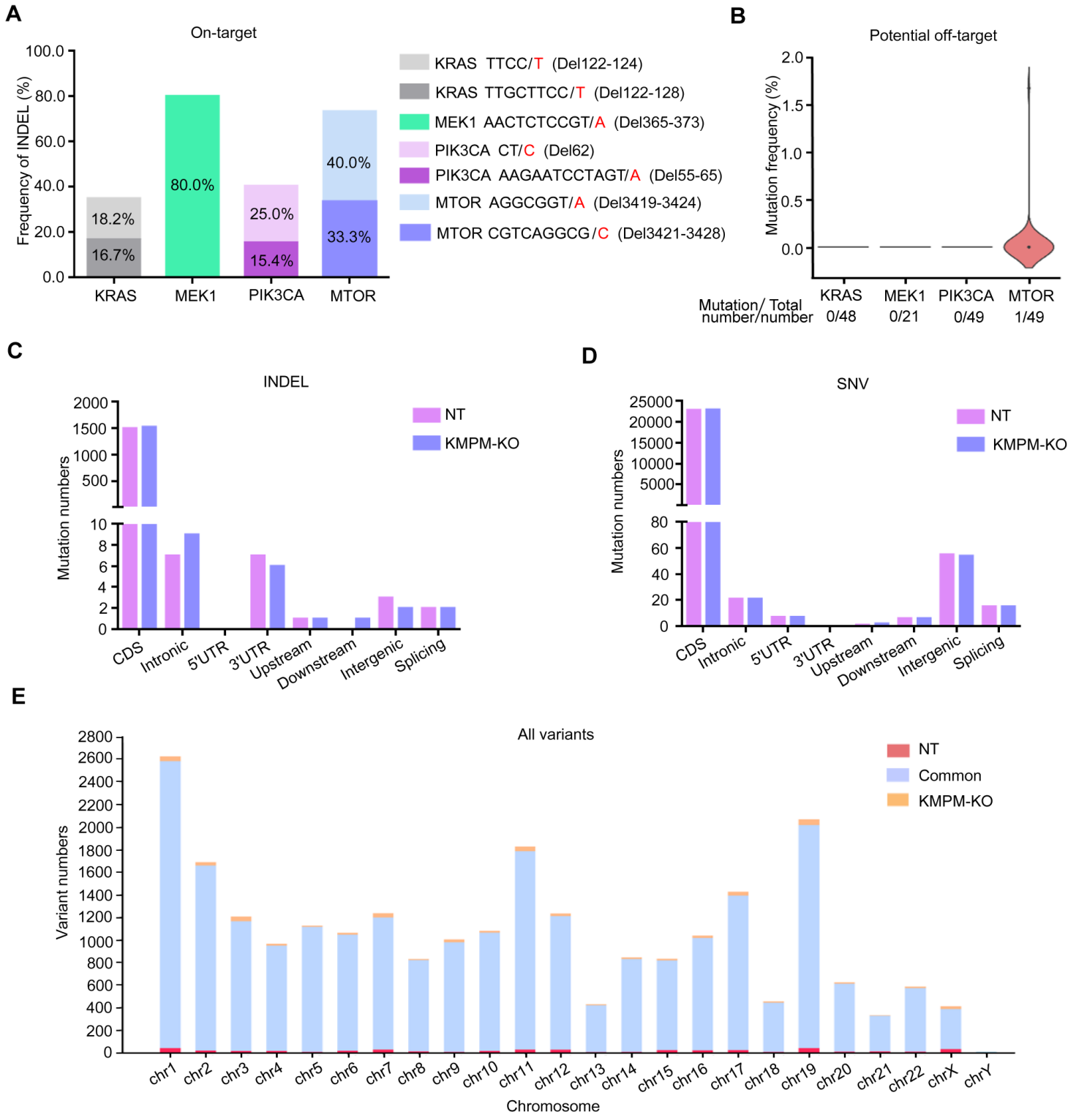

Figure 8

The on-target and off-target mutations in tumor tissues with quadruple-editing (A). On-target mutations detected by WES sequencing in tumor tissues of HCT116 CDX model with quadruple-editing. Seven kinds of deletions were detected in the target regions of the four genes. Their mutation frequencies and locations were respectively presented in bar plots. (B). Off-target mutations detected at potential mutation sites in tumor tissues of CDX mice with quadruple-editing. The frequencies of off-target mutations of the four target genes were respectively presented in violin plots. The total numbers of potential off-target sites predicted by Benchling tool and the numbers of real mutations detected by WES were listed below the graphs. (C-D). The numbers of INDEL (C) and SNV (D) detected at different genomic regions in tumor tissues of CDX mice with quadruple-editing and in control tumor tissues. (E). The variation numbers detected at different chromosomes in tumor tissues of CDX mice with quadruple-editing and in control tumor tissues. The numbers of common and unique variants in the tumor tissues of control and quadruple-editing were respectively presented in bar plots.

Supplementary Files

This is a list of supplementary files associated with this preprint. Click to download.

- AdditionalFile1TableS1S3.docx
- AdditionalFile2FigureS1.docx
- AdditionalFile3FigureS2.docx
- AdditionalFile4FigureS3.docx
- AdditionalFile5FigureS4.docx
- AdditionalFile6FigureS5.docx